Biomass Conversion and Biorefinery (2024) 14:5999–6010
https://doi.org/10.1007/s13399-021-01399-9

ORIGINAL ARTICLE

Utilization of prepared activated biochar from water lily (*Nymphaea lotus*) stem for adsorption of malachite green dye from aqueous solution

Jamiu Mosebolatan Jabar[1] · Yisau Adelaja Odusote[2]

Received: 30 November 2020 / Revised: 15 February 2021 / Accepted: 22 February 2021 / Published online: 1 March 2021

Abstract

Activated biochar was prepared from water lily through combination of physical and chemical technique. The prepared adsorbent was characterized by thermogravimetric analysis (TGA), elemental analysis (CHN/O), Fourier transform infrared spectrometry (FTIR), scanning electron microscopy (SEM), X-ray diffractometry (XRD), and Brunauer-Emmett-Teller model (BET). Batch technique was used for adsorption of 99.25% of MG dye onto prepared adsorbent with 102.35 mg/g maximum monolayer adsorption capacity (Q_{max}) at optimum conditions of initial dye concentration (100 mg/L), adsorbent dose (0.1 g/100 mL), contact time (30 min), temperature (301 K), and stirring speed (200 rpm). Kinetic and equilibrium models were best fit with pseudo-first order kinetic and Langmuir isotherm, respectively. Thermodynamic parameters showedΔH^o, ΔS^o, and ΔG^o to be 1.154 kJ/mol, 3.139 kJ/mol K, and −943.685 kJ/mol, respectively. Positive value of ΔH^o and large value of ΔS^o indicated that adsorption process was endothermic and that there was high collision rate at adsorbent–dye interface. The negative value of ΔG^oconfirmed that adsorption process was spontaneous and feasible. Comparison of water lily stem-derived activated biochar (WLSAB) Q_{max} with those reported for other plant-derived activated carbons affirmed WLSAB as a better potential alternative adsorbent for treatment of dye-contaminated wastewater.

Keywords Activated biochar, · Adsorbent dose, · Isotherm, · Spontaneous, · Wastewater

1 Introduction

Dyes and pigments are frequently used for coloration of materials to serve different purposes [1]. Most chemical and allied industries in developing nations that use dyes and pigments for decorating their products usually discharge their wastewater (effluent) directly into water bodies. The industry that contributes most to pollution of water bodies is textile industry due to use and discharge of large volume of water during its production process [2]. Other industries are cosmetic, agrochemical, pharmaceutical, food, leather, plastics, pulp, and paper industry [3]. Effluents from these industries hinder phytoplankton's photosynthesis, which confine aqua ecosystem [4].

Among the popular dyes used by textile industry in beautification of their products is malachite green dye (MG). Besides these economic benefits, MG dye also comes with its own demerits. Some of the demerits of MG dye in water bodies are reduction in appetite, growth, and fertility of aqua lives. In severe exposure, it may cause damage in vital organs, such as the heart, spleen, kidney, lung, skin, eye, and bone of the fish and other aqua lives. It may also lead to development of tumor and poisoning of the ovary, breast, and respiratory enzymes in mammals that feed on polluted water [5].

Removal of this dye from wastewater is mandatory to maintain the aquatic eco-balance and prevent silent death of mammals that use such polluted water for their industrial and/or domestic purpose. Unfortunately, MG dye is not completely removable from wastewater by conventional chemical (coagulation, precipitation, flocculation, ion exchange, etc.) and biological (aerobic, anaerobic, etc.) methods used by many researchers to remove

✉ Jamiu Mosebolatan Jabar
jmjabar@futa.edu.ng

[1] Textile and Polymer Research Laboratory, Chemistry Department, Federal University of Technology, P.M.B., Akure 704, Nigeria

[2] Condensed Matter and Statistical Physics, Department of Physics, Federal University of Technology, P.M.B., Akure 704, Nigeria

coloring matters from wastewater. It is only physical method (reverse osmosis, membrane separation, adsorption, etc.) of wastewater treatment that can remove this dye from wastewater completely without any challenge. Among the physical methods of wastewater treatment, adsorption is frequently used due to its simplicity, effectiveness, and environmental friendly [2]. The most popular process among adsorption methods of removing pollutants from wastewater involves the use of activated carbon [6]. High cost of commercially sold activated carbon motivated researchers in searching for agro-waste materials for production of low-cost effective activated carbon for treatment of wastewater [7]. Few of these agro-waste materials used in preparation of activated carbon are empty fruit bunch fiber [2], shell of cashew [8], *Persea americana* [9], *Ficus carica* bast [10], and coconut shell [11].

Water lilies are perennial aquatic ornamental plants [12]. These plants belong to order *Nymphaeale* and family and genus *Nymphaeaceae* and *Nymphaea*, respectively, with about fifty-eight (58) different species found on freshwaters (such as ponds, streams, and rivers) in temperate and tropical regions throughout the world [13]. There is limited information on the use of water lily for wastewater treatment. The little available information were on its leaf, seed, and root for removal of heavy metals from wastewater with very low maximum monolayer adsorption capacities [14, 15]. The use of water lily stem for removal of dye from aqueous solution has not been reported to the best of our knowledge. In western part of Nigeria, the mostly found specie of these plants is *Nymphaea lotus* with bluish green waxy coated round tender leaves. It has fragrant, cuplike flower above water surface on stalk that is attached to the underground stem with spiral arrangement of numerous petals. The leaves and shoot of water lily are used for treatment of kidney disease, catarrh, diarrhea, and bronchial infection. The fibrous root and berrylike seed are used for curing ulcer, cuts, wounds, and painful swollen boils. Other uses of this plant are tea bag, soap, and cream production [14].

Nymphaea lotus is underutilized in Nigeria as it widely spreads on water bodies covering virtually the entire surface of water, thereby contributing to environmental water drainage problem, reduction of dissolved oxygen, and sunlight penetration in freshwater. Utilization of *N. lotus* for production of activated biochar was aimed at converting aquatic weed to wealth through application of its biomass-derived adsorbent for removal of toxic MG dye from aqueous solution.

Statement of novelty The study has established possibility of converting aquatic weed (water lily stem) to wealth through its conversion to activated biochar (an economically friendly adsorbent) and utilization for adsorption of MG dye from aqueous solution.

2 Materials and methods

2.1 Materials

Water lily stem (WLS) was obtained from a stream at Iponna nla community, Adebowale bus stop, Akure South Local Government, Ondo State, Nigeria. The plant was authenticated by the Department of Crop, Soil and Pest Management, the Federal University of Technology, Akure. Malachite dye stuff and other chemical reagents used were acquired from Sigma-Aldrich Chemie, Germany.

2.2 Preparation and characterization of adsorbent

Washing of WLS was done with the use of distilled water to get rid of mud, sand, and other associated impurities. WLS was then oven dried at 110°C for 5 h, ground, and sieved to particle size between 80 and 100 μm. Dried WLS (150 g) was charred through soaking in a round bottom flask (2 L) containing 98% sulfuric acid (300 mL) for 18 h at room temperature (28°C) to form water lily stem biochar (WLSB). Distilled water (600 mL) was introduced into WLSB–acid mixture and refluxed for 3 h. After refluxing period, the mixture was cooled, emptied into distilled water (2 L) in a glass vessel before being filtered, and oven dried at 110°C for 3 h [10]. WLSB was physically activated in a furnace by raising the temperature of WLSB in furnace to 750°C within 1 h at heating rate of 50°C min^{-1} under nitrogen atmosphere at flow rate of 150 mL min^{-1}. The furnace was allow to cool to 650°C at rate of 50°C min^{-1} before nitrogen gas was switched to oxygen gas at flow rate 50 mL min^{-1}; the biochar was activated by holding it at this condition for 20 min. The physically activated WLSB was soaked in NaOH (0.1 M) at liquor ratio 1:2 for 6 h and thoroughly washed with distilled water after the reaction period to neutralize any acidic or/and alkaline remnant(s) in water lily stem activated biochar (WLSAB) and dried to constant weight in oven at 110°C for 3 h [2]. Yields of the WLSB and WLSAB were determined from mass of dried biochar and mass of dried WLS (Eq. 1). WLSAB was further ground and sieved to particle size between 40 and 50 μm, characterized by thermogravimetric analysis (TGA), elemental analysis (CHN/O), Fourier transform infrared spectroscopy (FTIR), scanning electron microscopy (SEM), X-ray diffractometry (XRD), Brunauer-Emmett-Teller method (BET), and point of zero charge (pH_{pzc}).

$$Biochar\ yield\ (\%) = \left(\frac{mass\ of\ biochar\ (g)}{mass\ of\ dried\ WLS\ (g)}\right) x\ 100 \quad (1)$$

2.3 Preparation and standardization of adsorbate

MG dye stock solution (100 mg/L) was prepared according to previous study [2]. MG dye solution was standardized by scanning absorption spectrum and plotting calibration curve of the dye solution (varied from 20 to 100 mg/L) for each of the pH values (1–9) using UV–visible spectrophotometer (Pharmacia LKB Biochrome 4060) at each of the corresponding $_{max}$ to take care of variation in color of MG dye solution as pH value varied. The calibration curve plotted for each of the pH values was used for interpolation of adsorbed MG dye onto WLSAB at the corresponding pH value. The interpolated adsorbed MG dye was used to calculate true percentage MG removed and adsorption capacity of WLSAB at each of the pH values.

2.4 Adsorption experiments

The optimum MG dye removal from aqueous solution (100 mL) was evaluated through batch adsorption process. Adsorption parameters such as pH, initial dye concentration, adsorption dose, time, and temperature were varied to establish optimum conditions for dye uptake (Eq. 2) and percentage MG dye adsorbed (Eq. 3) from aqueous solution. After each of the adsorption processes, dye aliquot was decanted, centrifuged at 3000 rpm for 10 min and 1 mL of effluent taken with siring, and analyzed with UV–visible spectrophotometer [16].

$$q_e = \frac{(C_1 - C_2)v}{w} \tag{2}$$

$$R\,(\%) = \frac{(C_1 - C_2)100\%}{C_1} \tag{3}$$

where q_e (mg/g) is the MG dye uptake, $C_1$and C_2 (mg/L) are the MG dye concentrations before and after adsorption process, respectively, v (mL) is the volume of MG dye solution, and w (g)e is the weight of WLSAB (adsorbent).

2.5 Regeneration studies

WLSAB reusability as adsorbent for removal of MG dye from aqueous solution was evaluated according to Choudhary et al. [17].

3 Results and discussion

3.1 Characterization of WLSAB

Table 1 shows yield of the prepared WLSAB adsorbent to be relatively high compared to yields of activated biochars from biomass reported by some researchers [18, 19]. This observation confirmed possibility of preparing WLSAB adsorbent to industrial scale.

Thermostability of WLSAB before and after MG dye adsorption was carried out on thermogravimetric analyzer (Shimadzu TG 50, Japan) operated from 25 to 800 °C at heating rate of 10 °C min^{-1} under nitrogen gas and from 800 to 900 °C under oxygen gas for determination of ash content [20]. TGA thermograms for WLSAB before and after adsorption process show three and four degradation stages, respectively (Fig. 1a). The first degradation stage from 25 to 286°C and 25 to 319.33°C was associated with evaporation of moisture in WLSAB before and after adsorption with weight loss of 5.99 and 5.10 g, respectively. The second weight loss (35.29%) between 319.33 and 387.78°C could be linked to the decomposition of MG dye from MG dye-loaded WLSAB. The weight loss of 74.46 and 52.46% at 790.83 and 799.40°C, respectively, corresponds to the second and third degradation stages in WLSAB before and after MG adsorption from aqueous solution, respectively. This degradation stage could be due to elimination of volatile organic compounds and partial decomposition of the carbonaceous matrix. The last degradation stage from 790.83 to 900°C could be linked to the carbon skeleton decomposition under the oxygen atmosphere. The TGA residues (8.78 and 6.14%) of WLSAB at 900 °C were inorganic ash composition of the adsorbent before and after adsorption, respectively.

Elemental analysis (carbon, hydrogen, and nitrogen contents) of WLSAB before and after adsorption was carried using CHN analyzer (PerkinElmer) at 1800°C, while oxygen content was assessed at 1400°C under nitrogen environment [21]. Prior to adsorption process, WLSAB displayed C, N, H, and O contents to be 79.97, 1.35, 1.45, and 17.23%, respectively. However, after the adsorption process, carbon content reduced to 42.37%, while O, H, and N contents of WLSAB increased to 50.52, 5.39, and 1.72%, respectively. These observations might be due to oxygenation, hydration, and/or adsorption of MG dye from aqueous solution according to Thue et al. [22].

Facial functional groups in WLSAB before and after adsorption were identified using FTIR spectrophotometer (PerkinElmer) operated between wavenumber 500 and 4000 cm^{-1} (Fig. 1b). The broad spectrum at 3262 cm^{-1} could be traced to presence of OH and/or N–H functional groups in carbonaceous biomass according to previous study [2]. C–H asymmetric and symmetric stretching appeared at 2954 and 2856 cm^{-1}, respectively [4]. The characteristic peak at 1713 could be assigned to carbonyl (C=O) [8], while band at 1510 cm^{-1} confirmed amines (C–N) functional group in WLSAB [23]. The bands at 1212 and 1079 cm^{-1} confirmed the presence of C–O of organic moieties and moisture, respectively, in the

Table 1 Comparison of WLSAB yield with those of other plant-derived biochars for wastewater treatment

Biochar	WLSB	WLSAB	BC	ABC	M650b	A650b	Biochar B
Yield (%)	62.13	47.15	51.28	42.85	32.30	26.90	32.25
Reference	This work	This work	[17]	[17]	[18]	[18]	[19]

WLSB is water lily biochar, WLSAB is water lily activated biochar, BC is biochar, ABC is activated biochar, M650b is marabou bark charred at 650°C and A650b is aspen bark charred at 650°C

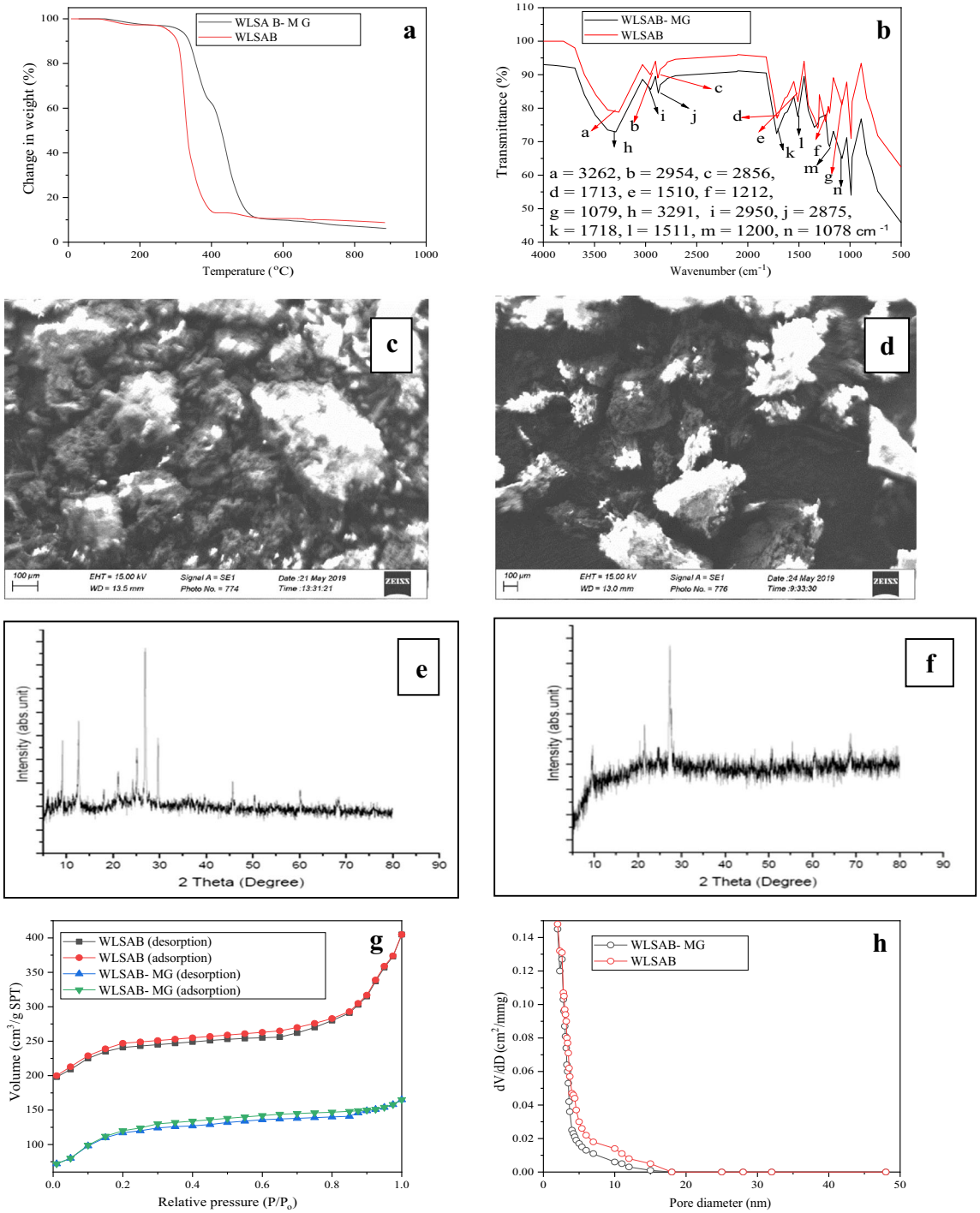

Fig. 1 **a** TGA thermograms, **b** FTIR spectra, **c**, **d** SEM images, **e**, **f** XRD spectra, and **g**, **h** N_2 adsorption-desorption isotherms and pore diameters of WLSAB adsorbent before and after MG dye adsorption from aqueous solution

prepared adsorbent [7]. Shift in all absorption bands observed in WLSAB after adsorption process confirmed MG dye adsorption onto WLSAB according to previous study [2].

The surface morphologies of WLSAB before and after adsorption were analyzed using scanning electron microscope. Figure 1c shows SEM image of WLSAB before adsorption to rough with cavities of different pore sizes and shapes for adsorption of MG dye from aqueous solution. Migration of MG dye molecules from aqueous solution onto the WLSAB matrix occurred by film diffusion through the cavities. The smooth surface of WLSAB after adsorption (Fig. 1d) was an affirmation of adsorption of MG dye onto the WLSAB. Similar results were reported by Yu et al. [24] and Hameed and El-Khaiary [25].

The X-ray diffraction patterns of WLSAB before and after adsorption were studied using X-ray diffractometer (Rigaku Dmax 7000). Figure 1e shows sharp peak of WLSAB (before adsorption) at 2 = 25.5° indicating amorphous carbon of carbonaceous material. Other peaks in the diffractogram are located at angles 9, 13, 22, 28, 46, 51, and 60.5°. However, after adsorption (Fig. 1f), the diffuse appearance and disappearance of some of the adsorbent peaks confirmed adsorption of MG dye onto WLSAB. Similar results were obtained by Liu et al. [26] in carbons prepared by pyrolysis of epoxy resins.

Nitrogen sorption isotherms studies were carried out to assess surface area, pore volume, pore diameter, and particle size distribution of WLSB and WLSAB (before and after adsorption) using gas sorption analyzer (ASAP 2420, USA) at −196°C. Isotherm sorption and pore size distribution curves of WLSB followed the same trend as that of WLSAB (before adsorption) shown in Fig. 1g and h, respectively. Those of WLSAB (after adsorption) were equally shown in Fig. 1g and h. The reduction of type IV isotherm of WLSAB to type II after adsorption indicated removal of MG dye from aqueous solution by the adsorbent. Equally, reduction of WLSAB specific surface area, total pore volume, average pore diameter, and increase in particle size distribution (Table 2) after adsorption process were further confirmation of adsorption of MG dye onto WLSAB. Similar results were reported by Choudhary et al. [17] in adsorption of MG dye onto *Opuntia ficus-indica*–activated biochar.

The electronic neutrality of WLSAB as adsorbent was evaluated according to previous study [16]. Figure 2a shows WLSAB pH_{pzc} to be 7.04; this implied that surface of WLSAB was mostly negatively charged at pH ≥ 7 and mostly positively charged at pH < 7 in MG dye solution. Therefore, more of MG dye molecules would be expected to be adsorbed from solution onto WLSAB at pH ≥ 7 due to electrostatic effects. At pH < 7, electrostatic repulsion might occur between cationic MG dye molecules and cationic surface charged WLSAB matrix. These observations are in line with Arfi et al. [27].

Table 2 Pore structural analysis of WLSB, WLSAB, and MG-WLSAB

Parameter	Unit	Biochar		
		WLSB	WLSAB	MG-WLSAB
S_{BET}	(m^2/g)	238.33	653.21	168.35
S_{total}	(m^2/g)	145.95	354.34	119.71
$S_{external}$	(m^2/g)	92.38	298.87	48.64
V_{total}	(m^3/g)	0.32	0.62	0.21
$V_{micropores}$	(m^3/g)	0.00	0.13	0.00
$V_{mesopores}$	(m^3/g)	0.32	0.49	0.21
$D_{average}$	(nm)	4.89	6.72	2.81
$D_{micropores}$	(nm)	1.07	1.25	1.08
$D_{mesopores}$	(nm)	3.82	5.47	1.73
Particle size	(mm)	0.049	0.044	

S_{BET} is specific surface area, S_{total} is total surface area, $S_{external}$ is external surface area, V_{total} is total pore volume, $V_{micropores}$ is micropores volume, $V_{mesopores}$ is mesopores volume, $D_{average}$ is average pore diameter, $D_{micropores}$ is micropores diameter, and $D_{mesopores}$ is mesopores diameter

3.2 Batch adsorption studies

3.2.1 Effect of pH on MG dye adsorption

pH played a major role in adsorption of MG dye onto WLSAB from aqueous solution. The MG dye adsorption mechanism was investigated through a range of pH from 1 to 9 at constant temperature (301 K), contact time (30 min), initial dye concentration (100 mg/L), adsorbent dose (0.1 g/100 mL), and stirring speed (200 rpm).

In the aqueous medium, MG dye ionized to form cationic moiety and at pH < 7, the surface of WLSAB was protonated (Scheme 1) according to pH_{pzc}. The lowest percentage MG dye removed at pH 1 might be due to strong electrostatic repulsion between the protonated WLSAB and cationic MG dye (Scheme 2a). WLSAB surface protonation relaxed as pH of dye medium increased from 1 to 6; hence, the percentage MG dye adsorbed from aqueous solution increased (Fig. 2b). These observations agreed with Yu et al. [24].

The reappearance of anionic functional groups (–OH, –C=O, –C–O, and –NH) on surface of WLSAB at pH ≥ 7 (according to pH_{pzc}) created electrostatic attraction between the anionic adsorbent and cationic adsorbate (Scheme 2b) according to findings made by Hameed and El-Khaiary [25] in adsorption of MG on oil palm trunk fiber.

Increase in percentage removal of MG dye from aqueous solution from pH 7 to 9 was insignificant. This observation agreed with findings of some researchers on adsorption of MG dye from aqueous solution using activated carbon [28–31]. Therefore, pH 7 was chosen as optimum and other adsorption processes were carried out at pH 7.

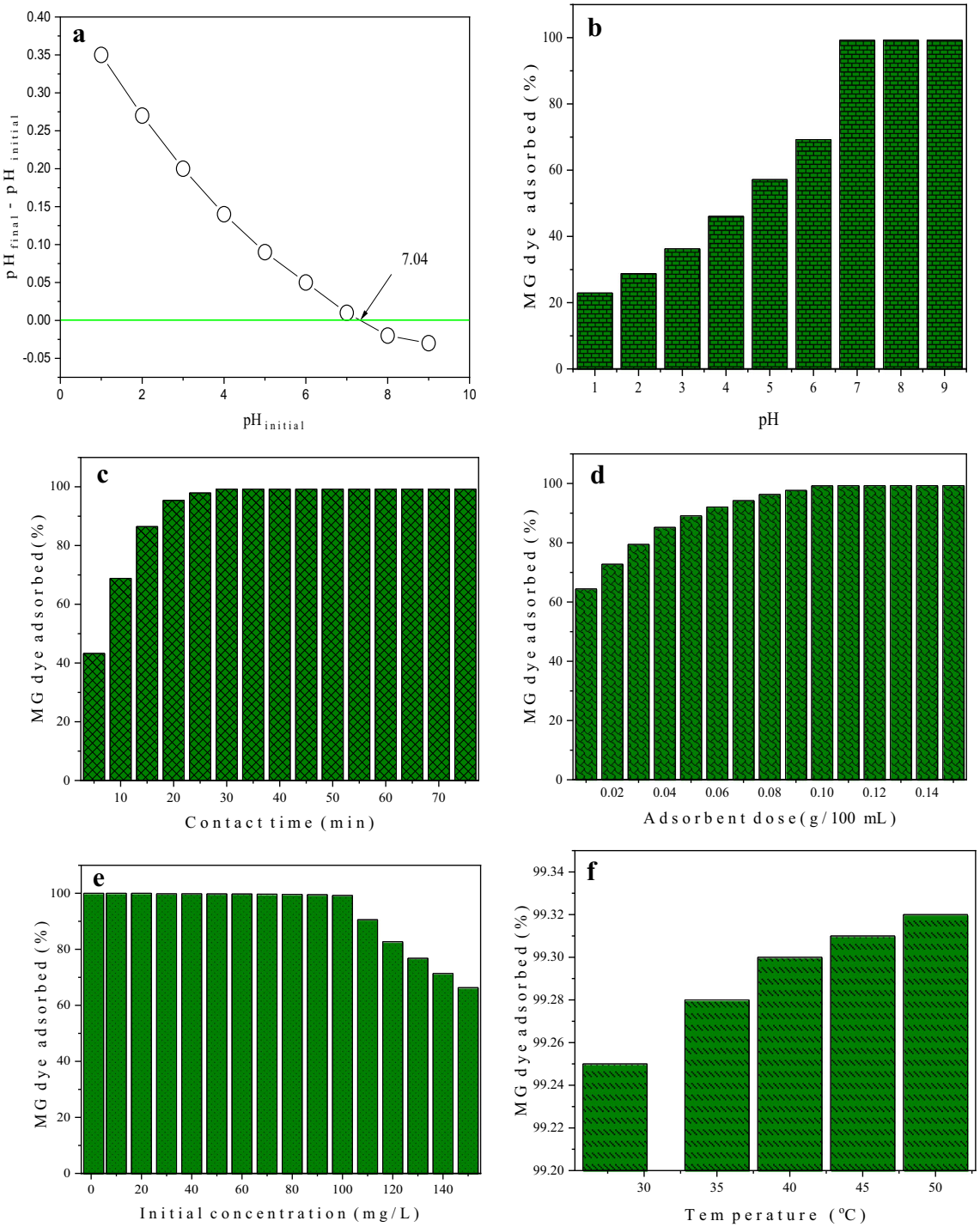

Fig. 2 **a** Point zero charge (pH_{pzc}), effect of **b** pH, **c** contact time, **d** adsorbent dose, **e** initial dye concentration, and **f** temperature on percentage MG dye adsorbed onto WLSAB

Scheme 1 **a** Ionization of MG dye in aqueous medium and **b** protonation of WLSAB in acidic medium

$$\text{Dye–Cl} \xrightarrow{\text{aqueous medium}} \text{Dye}^{+} + \text{Cl}^{-} \quad \text{(a)}$$

$$\text{WLSAB–OH} \xrightarrow[\text{pH} < 7]{\text{acidic medium}} \text{WLSAB}^{+} + \text{OH}^{-} \quad \text{(b)}$$

Scheme 2 **a** Electrostatic repulsion between MG dye and WLSAB and **b** electrostatic attraction of MG dye to WLSAB

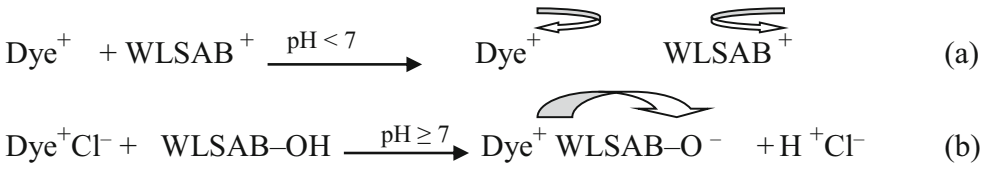

3.2.2 Effect of contact time on MG dye adsorption

Contact time is one of the economic factors to be considered for the selection of a particular adsorbent for treatment of wastewater. Evaluation of effect of contact time was done by varying the contact time from 5 to 75 min (5 min interval) at steady temperature (301 K), pH (7), initial dye concentration (100 mg/L), adsorbent dose (0.1 g/100 mL), and stirring speed (200 rpm).

Figure 2c shows rapid increase in percentage MG dye adsorbed onto WLSAB as contact time increased from 5 to 30 min; this observation is similar to the one made in the previous study [16]. Thereafter, there was negligible increase in percentage dye adsorbed as contact time increased to 75 min. This observation might be due to availability of virtually all active sites on WLSAB for binding MG dye from liquid phase at beginning of adsorption process up to 30 min. After which, most of the active sites got filled up and the remaining few unoccupied ones were difficult to access by dye molecules [32]. Optimum contact time of 30 min was used for other adsorption processes.

3.2.3 Effect of initial dye concentration and adsorbent dose on MG dye adsorption

Initial dye concentration and adsorbent dose are also factors that influence adsorption of MG dye onto WLSAB from aqueous solution.

The influence of adsorbent dose on MG removal efficiency was investigated by varying adsorbent dose from 0.01 to 0.15 g/100 mL at fixed temperature (301 K), contact time (30 min), pH (7), initial dye concentration (100 mg/L), and stirring speed (200 rpm).

It can be seen from Fig. 2d that as adsorbent dose increased from 0.01 to 0.10 g/100 mL, percentage MG dye adsorbed onto WLSAB increased. Increase in WLSAB quantity and available active sites for binding MG dye from aqueous solution might responsible for this observation according to Arfi et al. [27]. Negligible change in percentage MG dye adsorbed onto WLSAB was noticed as adsorbent dose increased from 0.10 to 0.15 g/100 mL. This might be as a result of great reduction in MG dye diffusion rate from liquid phase to solid phase due to high ratio of adsorbent dose to MG dye concentration according to previous study [2]. Therefore, adsorbent dose of 0.10 g/100 mL was used for other adsorption processes.

Varying initial dye concentration (1.0–150 mg/L) at constant temperature (301 K), contact time (30 min), pH (7), adsorbent dose (0.1 g/100 mL), and stirring speed (200 rpm) has a noticeable effect on dye removal from initial concentration of 1.0–100 mg/L (Fig. 2e). Although a noticeable change in percentage MG dye adsorbed onto WLSAB was not observed above initial concentration of 100 mg/L, the quantity of dye adsorbed onto WLSAB increased as initial concentration increased. These observations might be as a result of the low ratio of MG dye concentration to WLSAB available binding sites at low initial dye concentration and enhancement in interaction between the WLSAB available binding sites and MG dye molecules as initial concentration increased [29]. Initial dye concentration of 100 mg/L was chosen as optimum and used for other adsorption processes.

Table 3 Kinetic parameters for adsorption of MG dye onto WLSAB at varied time of adsorption

Parameter	Pseudo-first order	Pseudo-second order	Elovich
$q_{e\ (exp)}$ (mg/g)	99.250	99.250	99.250
$q_{e\ (cal)}$ (mg/g)	100.201	111.400	-
A_E (g/mg)	-	-	0.05
k_1 (min^{-1})	0.12353	-	-
k_2 (g/mg min)	-	0.00163	-
B_E (mg/g min)	-	-	74.178
SD (mg/g)	1.76068	4.901748	7.7095
R^2_{adj}	0.99595	0.96865	0.96370

3.2.4 Effect of temperature on adsorption of MG dye

Extent of energy consumption for wastewater treatment in adsorption process is another economic factor to be considered by industrialists in designing treatment plant. In estimating extent of heat required for optimum removal of MG dye from aqueous solution, temperature was varied from room temperature (301 K) to 323 K. Other parameters, such as adsorbent dose (0.1 mg/100 mL), contact time (30 min), pH (7), initial dye concentration (100 mg/L), and stirring speed (200 rpm), were kept constant. Figure 2f shows a slight increase in percentage MG dye adsorbed onto WLSAB as temperature increased from 301 to 323 K (28–50°C). Therefore, very little or no energy

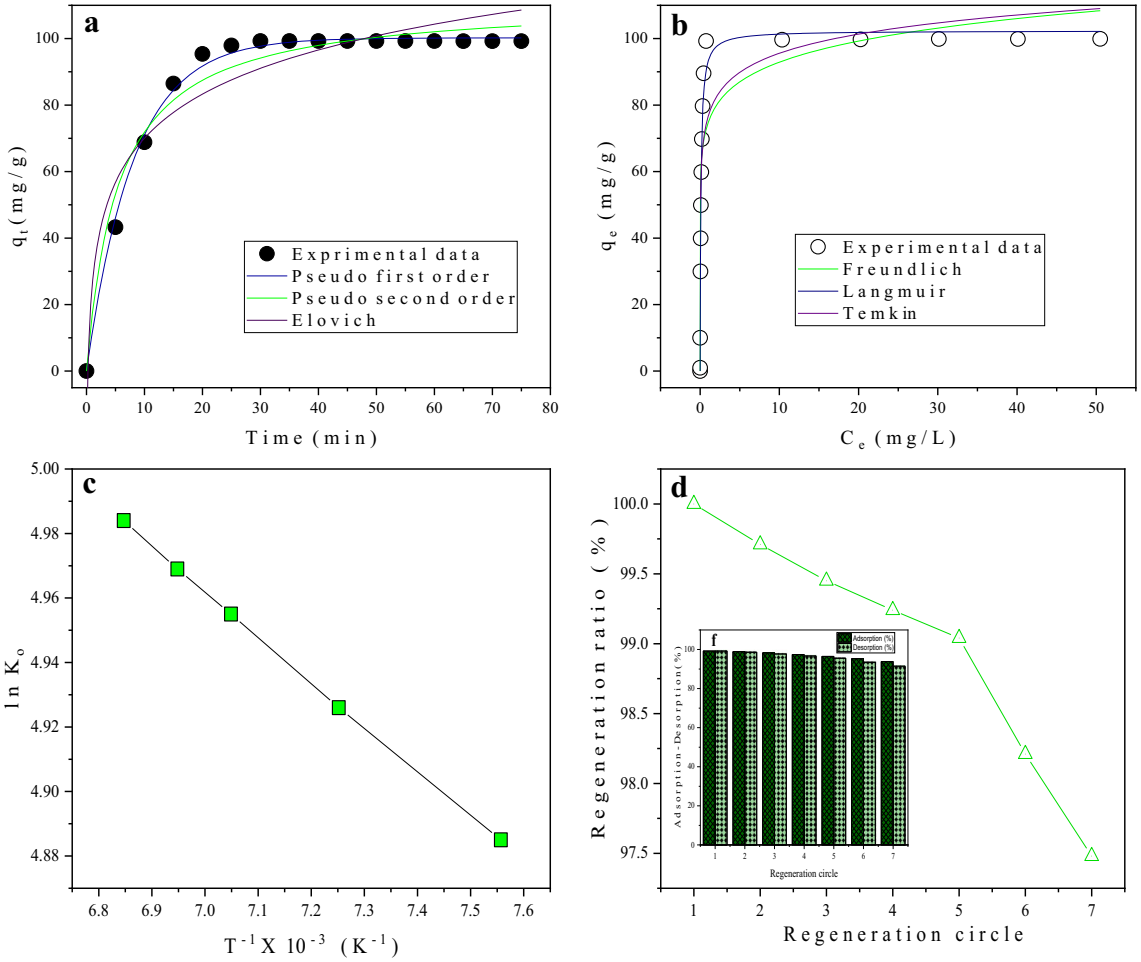

Fig. 3 **a** Kinetics, **b** isotherms, and **c** van't Hoff plot **d** regeneration ratio and **f** adsorption–desorption of adsorption of MG dye onto WLSAB

would be required for optimum treatment of wastewater containing MG dye using WLSAB as adsorbent by industrialists. This observation agreed with Hameed and El-Khaiary [25]. Other adsorption processes were carried out at room temperature (301 K).

3.3 Adsorption models

Data acquired from effects of variable parameters on MG dye adsorption onto WLSAB were used to investigate adsorption models.

Table 4 Isotherm parameters for adsorption of MG dye onto WLSAB at 301 K and different MG dye initial concentrations

Parameter	Langmuir	Freundlich	Temkin
Q_{max} (mg/g)	102.350	-	-
K_L (L/mg)	9.956	-	-
R_L	0.001	-	-
K_F (mg/g[L/mg]$^{1/n}$)	-	74.621	-
$\frac{1}{n}$	-	0.095	-
n	-	10.507	-
A_T (L/mg)	-	-	10031.260
B (mg/L)	*	-	8.300
b_T (J/mol)	-	-	301.500
SD (mg/g)	4.981343	13.678226	12.5003558
R^2_{adj}	0.995583	0.87707	0.89741

Table 5 Thermodynamic parameters for MG-WLSAB adsorption process at different temperatures

Temperature (K)	ΔH° (kJ mol^{-1})	ΔS° (kJ mol^{-1} K^{-1})	ΔG° (kJ mol^{-1})
301	1.154	3.139	-943.685
308	1.154	3.139	-965.658
313	1.154	3.139	-981.353
318	1.154	3.139	-997.048
323	1.154	3.139	-1012.740

3.3.1 Kinetic models

Nonlinear pseudo-first order (Eq. 4), pseudo-second order (Eq. 5), and Elovich (Eq. 6) kinetic models were used to study kinetic of adsorption of MG dye onto WLSAB.

$$q_t = q_e\left(1-e^{-k_1 t}\right) \tag{4}$$

$$q_t = \left(k_2 q^2{}_e t\right)/(1 + k_2 q_e t) \tag{5}$$

$$q_t = (1/A_E) ln(B_E\, A_E t) \tag{6}$$

where q_e and q_t (mg/g) are equilibrium dye uptake and dye uptake at a particular time; k_1 (min^{-1}) and k_2 (g/mg min) are pseudo-first and pseudo-second order rate constants, respectively. B_E (mg/g min) is the initial rate of adsorption and A_E (g/mg) is the extent of surface coverage in Elovich kinetic model.

Pseudo-first order model indicates adsorption process to be through physisorption (mechanical adhesion, van der Waal forces, or/and hydrogen bonding). Pseudo-second order and Elovich models indicate adsorption process to be through chemisorption (covalent forces, ion exchange, or/and sharing of electrons between adsorbent and adsorbate) [17]. The model with dye uptake calculated [$q_{e\ (cal)}$] most close to dye uptake experimented [$q_{e\ (exp)}$], lowest standard deviation (SD), and highest adjusted correlation coefficient ($R^2{}_{adj}$) is considered most fit [19].

The curves of the kinetic models are shown in Fig. 3a and the fitting parameters are presented in Table 1. The pseudo-first order model with highest $R^2{}_{adj}$, lowest SD, and most close $q_{e\ (cal)}$ to $q_{e\ (exp)}$ (Table 3) best fitted with kinetic model according to Thue et al. [8]. Similar observation was made by Hameed and El-Khaiary [21] in kinetic study of adsorption of MG on OPTF. This observation was an indication of adsorption of MG dye onto WLSAB being more controlled by physisorption mechanism.

3.3.2 Isotherm models

Concentration dependence data were used for nonlinear Freundlich (Eq. 7), Langmuir (Eq. 8), and Temkin equilibrium models (Eq. 9) to study adsorption isotherm.

$$q_e = K_F C_e{}^{1/n} \tag{7}$$

$$q_e = \frac{Q_{max} b C_e}{1 + K_L C_e} \tag{8}$$

$$q_e = B\ ln(A_T C_e) \tag{9}$$

K_L is related Langmuir dimensionless separation factor R_L (Eq. 10), which determines favorability of Langmuir isotherm.

$$R_L = \frac{1}{1 + K_L C_o} \tag{10}$$

b_T is obtainable from B as shown in Eq. 9.

$$B = \frac{RT}{b_T} \tag{11}$$

where K_F (mg/g[L/mg]$^{1/n}$) and n are Freundlich constants, K_L(L/mg) is the Langmuir equilibrium constant, Q_{max}(mg/g)

Table 6 Comparison of adsorption capacity of WLSAB with those of other plant-derived activated carbons for adsorption of MG dye from aqueous solution

Adsorbent	Q_{max}(mg/g)	Time (min)	pH	Temp. (K)	Reference
Nymphaea lotus (WLSAB)	102.35	30	7.0	301	This study
Limonia acidissima	34.56	210	7.5	299	[5]
Opuntia ficus-indica	1341.00	120	6.0	303	[17]
Cattail	210.18	360	8.0	303	[24]
Oil palm trunk fiber	149.35	115	5.0	303	[25]
Commercial activated carbon	8.27	240	7.0	303	[28]
Catha edulis	5.62	60	7.0	303	[29]
Ricinus communis epicarp	27.78	50	7.0	303	[30]
Arundo donax root	8.69	180	7.0	303	[31]
Borassus bark	20.70	40	6.0	303	[32]
Annona squamosa seed	25.91	100	6.0	300	[33]

is the maximum adsorption capacity of WLSAB, B (mg/L) and A_T (L/mg) are Temkin isotherm constants, b_T (J/mol) is the Temkin heat of sorption, R is the gas constant (8.314 J/mol K), and T (K) is the absolute temperature.

Isotherm curves of adsorption of MG dye onto WLSAB are shown in Fig. 3b and fitting parameters are presented in Table 4. The values of Langmuir dimensionless separation factor (R_L) and reciprocal of Freundlich constant (1/n) greater than 0 and less than 1 indicated that both adsorption models are feasible according to previous study [2]. Langmuir's model was the most suitable for describing the adsorption of MG dye onto WLSAB, because of its lowest value of SD and highest value of R^2_{adj} (Table 4). These observations established that the surface of WLSAB was homogeneous, adsorption of WLSAB on MG dye was monolayer, and adsorption was through chemical than physical process according to Santhi et al. [33]. This observation agreed with Sartape et al. [5]; Yu et al. [20]; and Santhi et al. [33] who are some of many researchers that also observed that adsorption of MG onto adsorbent was best fitted with Langmuir model.

3.3.3 Thermodynamic models

Adsorption thermodynamic was studied using van't Hoff expression (Eq. 12). Figure 3c presents van't Hoff plot obtained from plotting $\ln K_o$ against $^1/_T$ and Table 5 shows thermodynamic parameters.

$$\ln K_o = \frac{\Delta S^o}{R} - \frac{\Delta H^o}{R}\left(\frac{1}{T}\right) \tag{12}$$

where K_o is a ratio of dye uptake to MG dye effluent concentration, ΔS^o (kJ/mol K) is the entropy change, and ΔH^o (kJ/mol) is the adsorption enthalpy change.

ΔS^oandΔH^o were obtained from the intercept and slope of the graph. The positive value of ΔH^o indicated that adsorption process was endothermic. This observation was in line with Sartape et al. [5] in removal of MG from aqueous solution using WAS as low-cost adsorbent. Equally, magnitude ofΔH^o less than 40 kJ/mol established involvement of physisorption in adsorption process [2]. Gibb's standard free energy (ΔG^o) was obtained from values of ΔH^o and ΔS^o (Eq. 13).

$$\Delta G^o = \Delta H^o - T\Delta S^o \tag{13}$$

Large value of ΔS^o confirmed high collision rate at the WLSAB–MG dye interface during adsorption process, while negative value of ΔG^o established that adsorption process was spontaneous and feasible according to previous study [34, 35].

3.4 Comparison of adsorption capacity of WLSAB with other adsorbents

Maximum monolayer adsorption capacity (Q_{max}) of WLSAB is relatively high when compared with those reported for other plant-derived activate carbons in literature for adsorption of MG dye from aqueous solution (Table 6). Equally, WLSAB adsorbed MG dye from liquid phase faster than others reported in the literature. Therefore, WLSAB can be judged to be better than many activated carbons used by some researchers for removal of MG dye from aqueous solution.

3.5 Regeneration studies

Regeneration of WLSAB from MG-WLSAB was carried out through seven cycles of reusability study. Regeneration ratio greater than 97% (Fig. 3d) after seventh cycle regeneration process was an indication of WLSAB being a potential economical adsorbent for treatment of wastewater containing MG dye, other related dyes, and emerging contaminants. MG dye removal efficiency was equally observed from Fig. 3e to be greater than 91% after seventh adsorption-desorption process. This further confirmed that WLSAB is going to be an economic adsorbent for treatment of wastewater by the industrialists as it can be used several times before been deteriorated. Similar results were reported by Choudhary et al. [17].

4 Conclusion

WLSAB was successfully prepared from water lily stem and utilized for adsorption of MG dye from aqueous solution. Adsorption of MG dye onto WLSAB was confirmed through instrumental analyses. Adsorption of MG dye onto WLSAB was through both physisorption and chemisorption. It can be concluded that WLSAB was highly effective, because it adsorbed greater than 99% of MG dye from liquid phase within 30 min at room temperature. Therefore, this designed treatment plant will be economically friendly to the industrialists as very little or no external heat would be required for wastewater treatment within 30 min.

Acknowledgments The authors hereby acknowledge assistance rendered by Dr MA Adebayo of Chemistry Department, Federal University of Technology Akure, for the success of this research work.

Author' contributions Jabar JM provided the study concept and design; carried out materials preparation, data collection, and parts of analyses; and wrote the first draft of the manuscript, while Odusote YA carried out adsorbent regeneration studies and co-joined in preparation of the revised and current version of the manuscript. Both authors read and approved the final manuscript.

Declarations

Conflict of interest The author declares no competing interest.

References

1. Jabar JM, Ogunmokun AI, Taleat TAA (2020) Color and fastness properties of mordanted *Bridelia ferruginea* B dyed cellulosic fabric. Fash Text 7:1. https://doi.org/10.1186/s40691-019-0195-z
2. Jabar JM, Odusote YA (2020) Removal of cibacron blue 3G-A (CB) dye from aqueous solution using chemo-physically activated biochar from oil palm empty fruit bunch fiber. Arab J Chem 13: 5417–5429. https://doi.org/10.1016/j.arabjc.2020.03.020
3. Dhaif-Allah MAH, Taqui SN, Syed UT, Syed AA (2020) Kinetic and isotherm modeling for acid blue adsorption onto low-cost nutraceutical industrial fenugreek seed spent. Appl Water Sci 10:58. https://doi.org/10.1007/s13201-20-1141-3
4. Jabar JM, Odusote YA, Alabi KA, Ahmed IB (2020) Kinetics and mechanisms of congo-red dye removal from aqueous solution using activated *Moringa oleifera* seed coat as adsorbent. Appl Water Sci 10:136. https://doi.org/10.1007/s13201-020-01221-3
5. Sartape AS, Mandhare AM, Jadhav VV, Raut PD, Anuse MA, Kolekar SS (2014) Removal of malachite green dye from aqueous solution with adsorption technique using *Limonia acidissima* (wood apple) shell as low cost adsorbent. Arab J Chem 10: S3229–S3238. https://doi.org/10.1016/j.arabjc.2013.12.019
6. Lima TEC, Cardoso MG, Dias SLP, Pavan FA (2009) Application of carbon adsorbents prepared from the Brazilian-pine fruit shell for removal of Procion Red MX 3B from aqueous solution – kinetic, equilibrium and thermodynamic studies. Chem Eng J 155:627–636
7. Garg VK, Amita M, Kumar R, Gupta R (2004) Basic dye (methylene blue) removal from simulated wastewater by adsorption using Indian rosewood sawdust. Dyes Pigmns 63:243–250
8. Thue PS, Lima DR, Naushad M, Lima EC, de Albuquerque YRT, Dias SLP, Cunha MR, Dotto GL, de Brum IAS (2020) High removal of emerging contaminants from wastewater by activated carbons derived from the shell of cashew of Para. Carbon Lett. https://doi.org/10.1007/s42823-020-00145-x
9. Regti A, Laamari MR, Stiriba S, Haddad ME (2017) Removal of basic blue 41 dyes using *Persea americana*-activated carbon prepared by phosphoric acid action. Int J Ind Chem 8:187–195
10. Pathania D, Sharma S, Singh P (2017) Removal of methylene blue by adsorption onto activated carbon developed from *Ficus carica* bast. Arab J Chem 10:S1445–S1451. https://doi.org/10.1016/j.arabjc.2013.04.021
11. Aljeboree AM, Alshirrifi AN, Alkaim AF (2014) Kinetics and equilibrium study for the adsorption of textile dyes on coconut shell activated carbon. Arab J Chem. https://doi.org/10.1016/j.arabjc.2014.01.020
12. Chen F, Liu X, Yu C, Chen Y, Tang H, Zhang L (2017) Water lilies as emerging models for Darwin's abominable mystery. Hortic Res 4:17051. https://doi.org/10.1038/hortres.2017.51
13. Less DH, Schneider EL, Padgett DJ, Soltis PS, Soltis DE, Zanis M (1999) Phylogeny, classification and floral evolution of water lilies (Nymphaeaceae; Nymphaeales): a synthesis of non-molecular *rbcl, matK* and 185 rDNA data. Syst Bot 24:28–46
14. Galadima LG, Wasagu RSU, Lawal M, Aliero AA, Magaji UF, Suleman H (2015) Biosorption activity of *Nymphaea lotus* (water lily). Int J Eng Sci 3(4):66–70
15. Gongden JJ, Nnebedum J, Kagoro ML (2016) Kinetic and thermodynamic assessment of the adsorption of cadmium using water lily (Nymphaea ampla) leaf biomass. J Middle East North Afric Sci 2(10):1–9
16. Jabar JM, Owokotomo IA, Ayinde YT, Alafabusuyi AM, Olagunju GO, Mobolaji VO (2021) Characterization of prepared eco-friendly biochar from almond (*Terminalia catappa* L) leaf for sequestration of bromophenol blue (BPB) from aqueous solution. Carbon Lett. https://doi.org/10.1007/s42823-020-00214-1
17. Choudhary M, Kumar R, Neogi S (2020) Activated biochar derived from *Opuntia ficus-indica* for the efficient adsorption of malachite green dye, Cu^{2+} and $Ni^{2+}$from water. J Hazard Matter 392:122441. https://doi.org/10.1016/j.jhazamat.2020.122441
18. Idowu GA, Fletcher AJ (2019) The manufacture and characterisation of rosid angiosperm-derived biochars applied to water treatment. BioEnergy Res 13:387–396. https://doi.org/10.1007/s12155-019-10074-x
19. Adesmuyi MF, Adebayo MA, Akinola AO, Olasehinde EF, Adewole KA, Lajide L (2020) Preparation and characterization of biochars from elephant grass and utilization for aqueous nitrate removal: effect of pyrolysis temperature. J Environ Chem Eng 8: 104507. https://doi.org/10.1016/j.jece.2020.1045074
20. Lima DR, Hosseini-Bandegharaei A, Thue PS, Lima EC, de Albuquerque YRT, dos Reis GS, Umpierres CS, Dias SLP, Tran HN (2019) Efficient acetaminophen removal from water and hospital effluents treatment by activated carbons derived from Brazil nutshells. Colloids Surf A Physicochem Eng Asp 583:1–12
21. Kasperiski FM, Lima EC, Umpierres CS, dos Reis GS, Thue PS, Lima DR, Dias SLP, Saucier C, da Costa JB (2018) Production of porous activated carbons from *Caesalpinia ferrea* seed pod wastes: highly efficient removal of captopril from aqueous solutions. J Clean Prod 197:919–929
22. Thue PS, Lima EC, Sieliechi JM, Saucier C, Dias SLP, Vaghetti JCP, Rodembusch FS, Pavan FA (2017) Effects of first–row transition metals and impregnation ratios on the physicochemical properties of microwave-assisted activated carbons from wood biomass. J Colloid Interface Sci 486:163–175
23. de Oliveira Carvalho C, Rodrigues DLC, Lima EC, Umpierres CS, Caicedo DF, Machado FM (2019) Kinetic, Equilibrium, and thermodynamic studies on the adsorption of ciprofloxacin by activated carbon produced from Jerivá (*Syagrus romanzoffiana*). Environ Sci Pollut Res 26:4690–4702
24. Yu M, Han Y, Li J, Wang L (2017) CO_2-activated porous carbon derived from cattail biomass for removal of malachite green dye and application as supercapacitors. Chem Eng J 317:493–502. https://doi.org/10.1016/j.cej.2017.02.105
25. Hameed BH, El-Khaiary MI (2007) Batch removal of malachite green from aqueous solutions by adsorption on oil palm trunk fibre: equilibrium isotherms and kinetic studies. J Hazard Matter 154: 237–244
26. Liu Y, Xue JS, Zheng T, Dahn JR (1996) Mechanism of lithium insertion in hard carbons prepared by pyrolysis of epoxy resins. Carbon 34:193–200. https://doi.org/10.1016/0008-6223(96)00177-7
27. Arfi RB, Karou S, Mougin K, Ghorbal A (2017) Adsorptive removal of cationic and anionic dyes from aqueous solution by utilizing almond shell as bioadsorbent. Euro-Mediterr J Environ Integr 2:20. https://doi.org/10.1007/s41207-017-0032-y
28. Mall ID, Srivastava VC, Agarwal NK, Mishra IM (2005) Adsorptive removal of malachite green dye from aqueous solution by bagasse fly ash and activated carbon – kinetic study and equilibrium isotherm analyses. Colloids Surf A Physicochem Eng Asp 264(1–3):17–28
29. Abate GY, Alene AN, Habte AT, Getahun DM (2020) Adsorptive removal of malachite green dye from aqueous solution onto activated carbon of *Catha edulis* stem as a low cost bio-adsorbent. Environ Syst Res 9:29. https://doi.org/10.1186/s40068-020-00191-4
30. Santhi T, Manonmani S, Smitha T (2010) Removal of malachite green from aqueous solution by activated carbon prepared from the

epicarp of *Ricinus communis* by adsorption. J Hazard Mater 179: 178–186
31. Zhang J, Li Y, Zhang C, Jing Y (2008) Adsorption of malachite green from aqueous solution onto carbon prepared from Arundo donax root. J Hazard Mater 50:774
32. Arivoli S, Hema M, Martin P, Prasath D (2009) Adsorption of malachite green onto carbon prepared from Borassus bark. Arab J Sci Eng 34(2):31
33. Santhi T, Manonmani S, Vasantha VS, Chang YT (2011) A new alternative adsorbent for the removal of cationic dyes from aqueous solution. Arab J Chem 9:S466–S474. https://doi.org/10.1016/j.arabjc.2011.06.004
34. Adetuyi AO, Jabar JM (2010) Adsorption isotherm studies of indigo on some activated agro-solid wastes. Asian dyers 7(3):46 – 49
35. Adetuyi AO, Jabar JM (2011) Kinetic and thermodynamic studies of indigo adsorption on some activate bio-solids. J Chem Soc Pak 33(2):158–165